

# Evaluation of Thermal Gradient Mechanical Fatigue Characteristics of Thermal Barrier Coating, Considering the Effects of Thermally Grown Oxide

Jeong-Min Lee<sup>1</sup>, Hyunwoo Song<sup>1</sup>, Yongseok Kim<sup>1</sup>, Jae-Mean Koo<sup>2</sup>, and Chang-Sung Seok<sup>2,#</sup>

<sup>1</sup> Graduate School of Mechanical Engineering, Sungkyunkwan University, 2066, Seobu-ro, Jangan-gu, Suwon-si, Gyeonggi-do, 440-746, South Korea

<sup>2</sup> School of Mechanical Engineering, Sungkyunkwan University, 2066, Seobu-ro, Jangan-gu, Suwon-si, Gyeonggi-do, 440-746, South Korea

# Corresponding Author / E-mail: seok@skku.edu, TEL: +82-31-290-7446, FAX: +82-31-299-4866

KEYWORDS: Gas turbine blade, Thermal gradient mechanical fatigue, Low cycle fatigue, Finite element analysis

*Gas turbines of aircraft and power generation plants operate at a high turbine inlet temperature (TIT) or combustion temperature higher than 1,000°C to obtain high thermal efficiency. The parts directly in contact with the high temperature flame are made of a nickel-base superalloy, which has strong heat resistance. In addition, the thermal barrier coating (TBC) technique is applied to increase the heat resistance. The TBC prevents direct heat transfer from the high temperature flame to the metallic substrate. Thus, the TBC technique reduces the substrate surface temperature by approximately 100–170°C. The delamination caused by the growth of thermally grown oxide (TGO) decreases the life of the TBC system. In addition, gas turbine blades experience centrifugal forces owing to high speeds of approximately 3600 rpm and they experience low cycle fatigue because of frequent startup and shutdown. Therefore, the integrity of the TBC system should be evaluated under the thermal gradient mechanical fatigue condition. In this study, finite element analysis (FEA) was performed for the TBC model considering TGO, and the effect of TGO on TBC systems was evaluated under the thermal gradient mechanical fatigue condition.*

Manuscript received: July 22, 2014 / Revised: November 6, 2014 / Accepted: April 13, 2015

## NOMENCLATURE

$\varepsilon_{th}$  = thermal strain (%)

$\varepsilon_{mech}$  = mechanical strain (%)

$\varepsilon_{tot}$  = total strain (%)

## 1. Introduction

The first stage gas turbine blade is exposed to a high temperature flame of approximately 1,350°C. Therefore, thermal barrier coating (TBC) technology is applied to improve the durability. Thermal barrier coating consists of a top coat and a bond coat. The top coat protects the substrate from the flame and the bond coat increases the bonding strength between the top coat and the substrate.<sup>1-4</sup> Thermal stress is generated owing to the difference in the thermal expansion coefficients.

Gas turbine blades also experience mechanical loads from high-speed rotation of approximately 3,600 rpm. In addition, gas turbine blades experience low-cycle fatigue owing to frequent startups and shutdowns. They are operated under a harsh condition of thermal fatigue and mechanical fatigue. Microscopic cracks are generated by repeated thermal gradient mechanical fatigue and these cracks lead to delamination of the TBC system. Delamination of the TBC system causes rapid decrease in the life of the gas turbine blade because the substrate is directly exposed to the flame. Therefore, the integrity evaluation of the TBC system is necessary to evaluate the reliability of the gas turbine blades.<sup>5</sup>

During the gas turbine operation, thermally grown oxide (TGO) is generated between the top coat and the bond coat. By preventing oxygen from entering the substrate, TGO prevents the oxidation of the material. TGO also causes the microscopic cracks in the fatigue loading.<sup>6,7</sup> Also, the thickness of the TGO is increased, and the TGO is ruptured by temperature change or degradation. Thus, TGO is a very important factor that affects the life of the TBC system. To identify the

Table 1 Material properties of TBC system

	Top coat (8YSZ)	Bond coat (MCrAlY)	Substrate (IN738LC)	TGO ( $\text{Al}_2\text{O}_3$ )
Young's modulus (GPa)	53	156	225	364–416
Poisson's ratio	0.25	0.27	0.27	0.23–0.25
Density ( $\text{kg}/\text{m}^3$ )	6037	7711	7890	3868–3984
Specific heat ( $\text{J}/\text{kg}^\circ\text{C}$ )	500	628	456	755–1285
Thermal expansion coefficient ( $10^{-6}/^\circ\text{C}$ )	7.6–12.7	12–19.3	11.6–15.9	4.6–8.3
Thermal conductivity ( $\text{W}/\text{mK}$ )	1–2.3	11.6–25	11.8–25.4	6.7–33

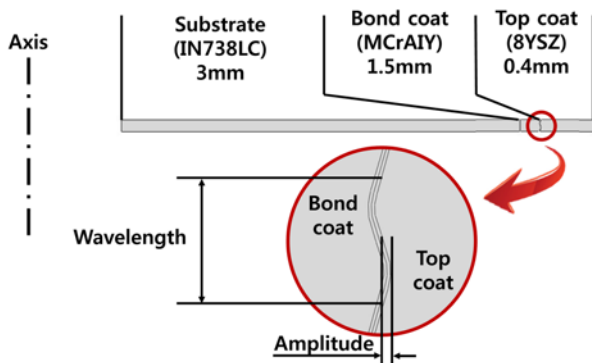


Fig. 1 Geometry of the specimen

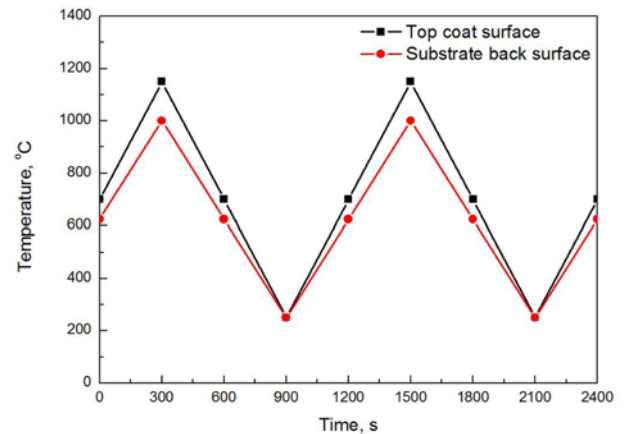


Fig. 2 Temperature condition in the FEA

TGO growth behavior according to the usage time and change in temperature, it is required to verify the reliability of the TBC system.

In this study, finite element analysis (FEA) of the TBC system was performed according to the amplitude of TGO. A relationship was found between the ratio of amplitude to wavelength of the TGO and the stresses seen in the top and bond coats.

## 2. Finite Element Analysis Model and Methods

### 2.1 Finite element analysis model

IN738LC is the main material used in the first-stage gas turbine blade and was used as a substrate in this study. 8YSZ and MCrAlY were used as the top coat and the bond coat, respectively. Because  $\text{Al}_2\text{O}_3$  is generated from the heat of the turbine, it was used as a model of TGO. The material properties of interest are summarized in Table 1.<sup>8–12</sup> FEAs were performed for the hollow shaft shape specimen, which is used in the thermal gradient mechanical fatigue test. TGO is generally modeled as sine wave form in the FEA. Thus, under the assumption of axisymmetric specimens, the FEA model was constructed in two dimensions like a Fig. 1, with the TGO period being only 1.5. The thicknesses of the substrate, top coat, and bond coat were 3 mm, 0.4 mm, 0.15 mm, respectively. TGO was set at a thickness of 0.004 mm and a wavelength of 0.06 mm. In addition, to simulate the rumpling of TGO, the analysis models were modeled for 5 cases with different ratio of the amplitude for the wavelength. The model consisted of 443,750 elements. The DCAX4 element type was used in the heat transfer analysis and the CAX4R element type was used in both the thermal deformation analysis and the thermo-mechanical fatigue analysis. To examine the generated stress according to the shape of TGO in the TBC system, FEAs were conducted under TGO amplitude changes.

### 2.2 Finite element analysis method

#### 2.2.1 Heat transfer analysis and thermal deformation analysis

First, heat transfer analysis was performed to derive the temperature distribution of the analysis model. As the temperature condition, the temperature of top coat was 1,150°C and the temperature of substrate was 1,000°C in the high temperature, and the temperatures of top coat and substrate were 250°C in the low temperature condition with reference to research of Kagawa et al.,<sup>13</sup> as shown in Fig. 2. FEA was consisted of 9 steps. In the first step, the temperature of the analysis model was maintained at the middle of the high temperature and the low temperature. In the other eight steps, high and low temperature boundary conditions were alternatively applied to simulate the thermo-mechanical fatigue condition for two cycles.

Thermal deformation analysis was performed to derive the thermal strain from the heat transfer analysis. The result of the heat transfer analysis was used as input data and the element type was changed to CAX4R. Considering the symmetry of the model, the bottom surface was fixed along the y-axis and the upper surface of the model was set to generate the same amount of deformation.

#### 2.2.2 Thermal gradient mechanical fatigue analysis

The total deformation that was used for thermal gradient mechanical fatigue analysis was obtained previously from the thermal deformation analysis. Total deformation was defined as the sum of thermal deformation and mechanical deformation. Thermal gradient mechanical fatigue analysis was performed to give a deformation condition for the upper surface of the analysis model as shown in Fig. 3. The result of the heat transfer analysis was used as input data. The same element type and model used for the thermal deformation analysis were used for

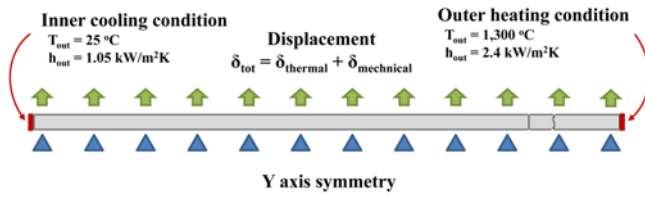


Fig. 3 Condition of finite element analysis

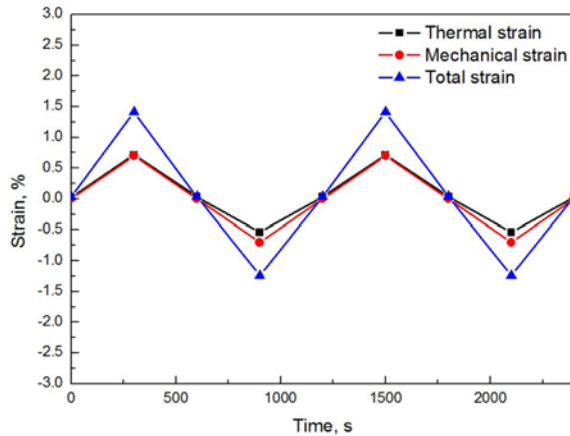


Fig. 4 Results of thermal deformation analysis

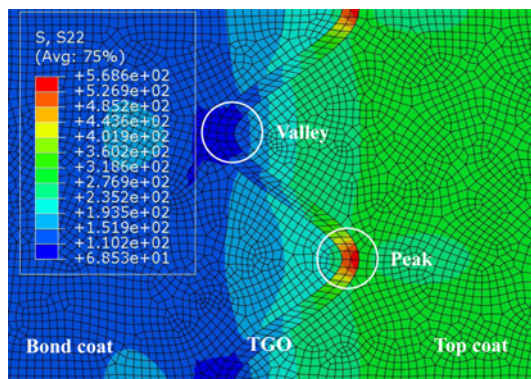


Fig. 5 Result of thermo-mechanical fatigue analysis under the high temperature and tension condition

the thermal gradient mechanical fatigue analysis. In this study, the mechanical strain was  $\pm 0.7\%$ . The reason of that is the maximum strain in the actual gas turbine is known as  $0.7\%$  in the operating condition. The thermal gradient mechanical fatigue analysis was performed in-phase, so that thermal fatigue and mechanical fatigue had the same phase.

### 3. Results of Finite Element Analysis

#### 3.1 Heat transfer analysis and thermal deformation analysis

The temperature distribution was obtained from the heat transfer analysis. The results showed a temperature difference of  $75^\circ\text{C}$  between the interface and the surface of top coat. Thermal deformation analysis

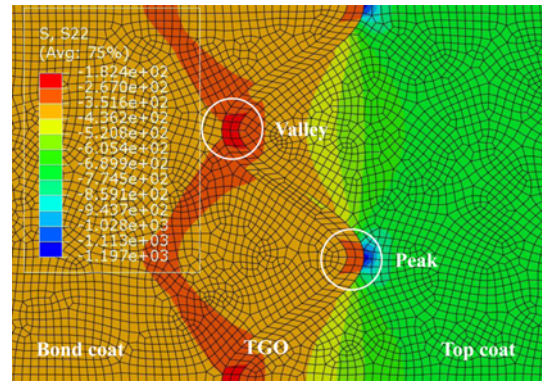


Fig. 6 Result of thermo-mechanical fatigue analysis under the low temperature and compression condition

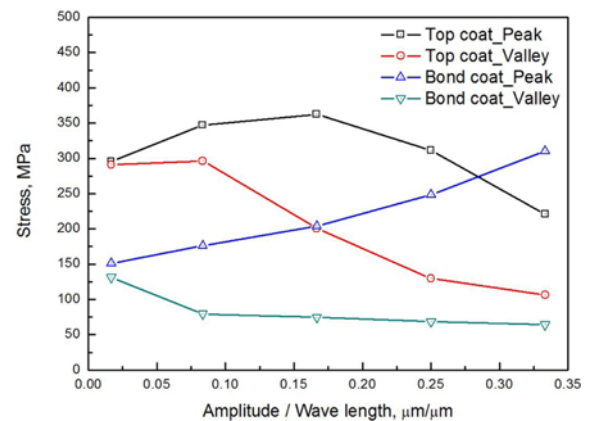


Fig. 7 Dependence of stress change on the ratio of TGO amplitude to wavelength under the high temperature and tension condition

was performed using the result of heat transfer analysis. Thermal strain was obtained according to the temperature at each step. The results of thermal deformation analysis are summarized in Fig. 4. The strain ratio was set to  $-1$ , and a triangular waveform was used.

#### 3.2 Thermal gradient mechanical fatigue analysis

The stress of the TBC system was obtained through a thermal gradient mechanical fatigue analysis of each step. According to the preceding research, fatigue life is determined by the amount of stress applied in the direction parallel to the coating layer. Thus, the stress parallel to the coating layer was derived in the TBC system.<sup>8</sup> The stresses that were generated in the top coat and the bond coat near the peak and valley of TGO were investigated to evaluate the effect caused by TGO. The results of analysis on the TGO were shown in Figs. 5 and 6.

### 4. Relationship between Stress and Ratio of Amplitude to Wavelength

#### 4.1 High temperature and tension condition

The result of the analysis under the high temperature and tension condition was shown in Fig. 7. The stresses in the TBC system were

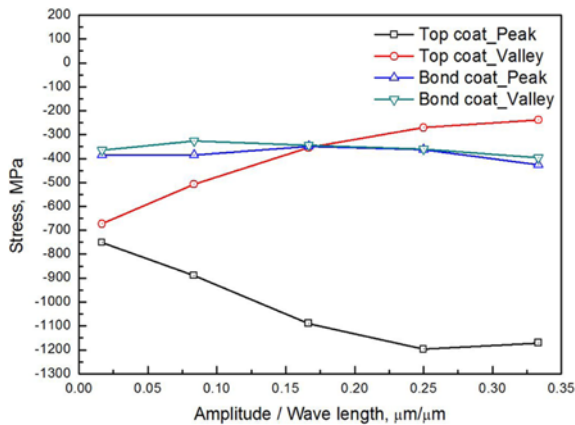


Fig. 8 Dependence of stress change on the ratio of TGO amplitude to wavelength under the low temperature and compression condition

affected by the ratio of the amplitude to wavelength. The tensile stress of the top coat near the peak was increased when the TGO amplitude was increased, but the stress was decreased once the ratio reached 0.15. For the top coat near the valley, the tensile stress was decreased owing to an increase in the TGO amplitude. An increase in the TGO amplitude resulted in an increase in the stress of the bond coat near the peak and a decrease in the stress of the bond coat near the valley.

#### 4.2 Low temperature and compression condition

The result of the analysis under the low temperature and compression condition was shown in Fig. 8. A large compressive stress, which was generated in the top coat near the peak and then decreased near the valley, was due to an increase in the TGO amplitude. The change of stress was smaller in the bond coat than in the top coat.

#### 4.3 Stress amplitude during fatigue

The stress range was defined as the difference between stress at the high temperature and stress at the low temperature. The stress amplitude was defined as one half of the stress range. The relationship between the stress amplitude and ratio of amplitude for the wavelength were shown in Fig. 9. The stress amplitude in the top coat near the peak was significantly increased but the stress amplitude in the top coat near the valley was decreased by an increase in the TGO amplitude. However, the stress amplitude did not change at bond coat. With an increase in the TGO amplitude, the top coat near the peak became weaker. Thus, it was expected that microscopic cracks would be generated in the top coat, which would lead to delamination.

### 5. Conclusions

In this study, thermo-mechanical fatigue analysis was performed for the TBC, which is used to improve the durability of first stage gas turbine blades. The stress in the TBC system was investigated according to the ratio of the TGO amplitude to wavelength. The conclusions of this study are as follows:

(1) The stress generated in the TBC system was caused by an increase in the TGO amplitude. The maximum tensile stress was

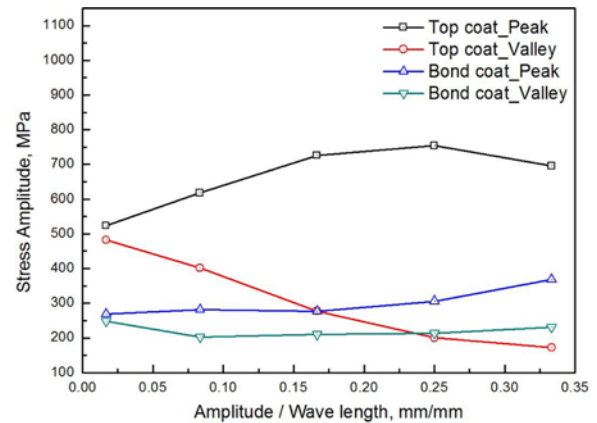


Fig. 9 Stress amplitude of TBC system

generated in the top coat near the peak under the high temperature and tension condition. The maximum compressive stress was also generated in the top coat near the peak under the low temperature and compression condition.

(2) The results obtained by deriving the stress amplitude for each location indicated that when the stress amplitude was significantly increased in the top coat near the peak, this area became weaker. Thus, it was expected that microscopic cracks would be generated in the top coat, which would lead to delamination.

### ACKNOWLEDGEMENT

This research was supported by Basic Science Research Program through the National Research Foundation of Korea (NRF) funded by the Ministry of Science, ICT & Future Planning (no. 2011-0020024).

### REFERENCES

- Kim, M. Y., Park, S. Y., Yang, S. H., Choi, H. S., Ko, W., et al., "Analysis of Damage Trend for Gas Turbine 1st Bucket Related to the Change of Models," *Transactions of the Korean Society of Mechanical Engineers A*, Vol. 31, No. 6, pp. 718-724, 2007.
- Shin, I. H., Lee, D. K., Koo, J. M., Seok, C. S., and Lee, T. W., "Evaluation of Failure Life of Thermal Barrier Coating applied Gas Turbine by Thermo-Mechanical Fatigue Test," *Proc. of KSPE Autumn Conference*, pp. 621-622, 2010.
- Lee, J. M., Seok, C. S., Lee, D., Kim, Y., Yun, J., et al., "Prediction of Thermo-Mechanical Fatigue Life of IN738LC using the Finite Element Analysis," *Int. J. Precis. Eng. Manuf.*, Vol. 15, No. 8, pp. 1733-1737, 2014.
- Kim, Y., Seok, C. S., Lee, S. Y., Koo, J. M., Kim, S. H., et al., "Development of Thermal Gradient Prediction Method for Thermal Barrier Coating," *Int. J. Precis. Eng. Manuf.*, Vol. 15, No. 6, pp. 1029-1033, 2014.
- Kim, D., Koo, J., Seok, C., Won, J., Park, S., et al., "Thermal

- Fatigue Test Methods for Thermal Barrier Coatings of Gas Turbine Blade,” J. Korean Soc. Precis. Eng., Vol. 26, No. 2, pp. 7-15, 2009.
6. Levi, C. G., Sommer, E., Terry, S. G., Catanoiu, A., and Rühle, M., “Alumina Grown During Deposition of Thermal Barrier Coatings on NiCrAlY,” Journal of the American Ceramic Society, Vol. 86, No. 4, pp. 676-685, 2003.
  7. Quadackers, W. J., Shemet, V., Sebold, D., Anton, R., Wessel, E., et al., “Oxidation Characteristics of a Platinized Meraly Bond Coat for TBC Systems During Cyclic Oxidation at 1000°C,” Surface and Coatings Technology, Vol. 199, No. 1, pp. 77-82, 2005.
  8. Koo, J. M. and Seok, C. S., “Design Technique for Improving the Durability of Top Coating for Thermal Barrier of Gas Turbine,” J. Korean Soc. Precis. Eng. Vol. 31, No. 1. pp. 15-20, 2014.
  9. Almeida, D., Silva, C., Nono, M., and Cairo, C., “Thermal Conductivity Investigation of Zirconia Co-Doped with Yttria and Niobia EB-PVD Tbc,” Materials Science and Engineering: A, Vol. 443, No. 1, pp. 60-65, 2007.
  10. Arnold, S. M., Pindera, M.-J., and Aboudi, J., “Analysis of Plasma-Sprayed Thermal Barrier Coatings with Homogeneous and Heterogeneous Bond Coats under Spatially Uniform Cyclic Thermal Loading,” NASA/TM-2003-210803, 2003.
  11. Ferguson, B., Petrus, G., and Krauss, T., “Modeling of Thermal Barrier Coatings,” NASA Contractor Report, Paper No. NAS-26664, 1992.
  12. Liu, A. and Wei, Y., “Finite Element Analysis of Anti-Spallation Thermal Barrier Coatings,” Surface and Coatings Technology, Vol. 165, No. 2, pp. 154-162, 2003.
  13. Kitazawa, R., Kakisawa, H., and Kagawa, Y., “Anisotropic TGO Morphology and Stress Distribution in EB-PVD  $Y_2O_3$ - $ZrO_2$  Thermal Barrier Coating after in-Phase Thermo-mechanical Test,” Surface and Coatings Technology, Vol. 238, pp. 68-74, 2014.